Research Article | Vol. 25, No. 5 | 6 Mar 2017 | OPTICS EXPRESS 4810

Optics EXPRESS

Ultra-flat wideband single-pump Raman-enhanced parametric amplification

V. GORDIENKO,* M. F. C. STEPHENS, A. E. EL-TAHER, AND N. J. DORAN

Aston Institute of Photonic Technologies, Aston University, Birmingham, B4 7ET, UK
**gordienv@aston.ac.uk*

Abstract: We experimentally optimize a single pump fiber optical parametric amplifier in terms of gain spectral bandwidth and gain variation (GV). We find that optimal performance is achieved with the pump tuned to the zero-dispersion wavelength of dispersion stable highly nonlinear fiber (HNLF). We demonstrate further improvement of parametric gain bandwidth and GV by decreasing the HNLF length. We discover that Raman and parametric gain spectra produced by the same pump may be merged together to enhance overall gain bandwidth, while keeping GV low. Consequently, we report an ultra-flat gain of 9.6 ± 0.5 dB over a range of 111 nm (12.8 THz) on one side of the pump. Additionally, we demonstrate amplification of a 60 Gbit/s QPSK signal tuned over a portion of the available bandwidth with OSNR penalty less than 1 dB for Q^2 below 14 dB.

OCIS codes: (190.4970) Parametric oscillators and amplifiers; (190.4410) Nonlinear optics, parametric processes.

References and links

1. M. E. Marhic, N. Kagi, T.-K. Chiang, and L. G. Kazovsky, "Broadband fiber optical parametric amplifiers," Opt. Lett. **21**(8), 573–575 (1996).
2. V. Gordienko, M. F. C. Stephens, S. Takasaka, A. E. El-Taher, I. D. Phillips, W. Forisyak, R. Sugizaki, and N. J. Doran, "Demonstration of an ultra-flat Raman-enhanced fibre optical parametric amplifier (FOPA) with >110nm gain-bandwidth," in *Proceedings of the 42nd European Conference and Exhibition on Optical Communications* (VDE, 2016), paper Th.2.P2.SC1.1.
3. R. Stolen and J. Bjorkholm, "Parametric amplification and frequency conversion in optical fibers," IEEE J. Quantum Electron. **18**(7), 1062–1072 (1982).
4. M. E. Marhic and G. K. P. Lei, "Hybrid fiber optical parametric amplifiers for broadband optical communication systems," in *Proceedings of IEEE International Conference on Transparent Optical Networks* (IEEE, 2014), paper Th.B2.4.
5. N. Shibata, R. P. Braun, and R. G. Waarts, "Phase-mismatch dependence of efficiency of wave generation through four-wave mixing in a single-mode optical fiber," IEEE J. Quantum Electron. **23**(7), 1205–1210 (1987).
6. M. E. Marhic, F. S. Yang, L. G. Kazovsky, and Y. Park, "Broadband fiber-optical parametric amplifiers and wavelength converters with low-ripple Chebyshev gain spectra," Opt. Lett. **21**(17), 1354–1356 (1996).
7. J. M. Chavez Boggio, J. D. Marconi, S. R. Bickham, and H. L. Fragnito, "Spectrally flat and broadband double-pumped fiber optical parametric amplifiers," Opt. Express **15**(9), 5288–5309 (2007).
8. J. M. C. Boggio, S. Moro, E. Myslivets, J. R. Windmiller, N. Alic, and S. Radic, "155-nm continuous-wave two-pump parametric amplification," IEEE Photonics Technol. Lett. **21**(10), 612–614 (2009).
9. J. M. C. Boggio, C. Lundström, J. Yang, H. Sunnerud, and P. A. Andrekson, "Double-pumped FOPA with 40 dB flat gain over 81 nm bandwidth," in *Proceedings of the 34th European Conference and Exhibition on Optical Communications* (IEEE, 2008), paper Tu.3.B.5.
10. M. E. Marhic, *Fiber Optical Parametric Amplifiers, Oscillators and Related Devices* (Cambridge University Press, 2008), Chap. 13.
11. T. Torounidis and P. Andrekson, "Broadband single-pumped fiber-optic parametric amplifiers," IEEE Photonics Technol. Lett. **19**(9), 650–652 (2007).
12. M. Jamshidifar, A. Vedadi, and M. E. Marhic, "Continuous-wave one-pump fiber optical parametric amplifier with 270 nm gain bandwidth," in *Proceedings of the 34th European Conference and Exhibition on Optical Communications* (IEEE, 2009), paper 1.1.4.
13. J. Kim, Ö. Boyraz, J. H. Lim, and M. N. Islam, "Gain enhancement in cascaded fiber parametric amplifier with quasi-phase matching: theory and experiment," J. Lightwave Technol. **19**(2), 247–251 (2001).
14. M. E. Marhic, F. S. Yang, M. Ho, and L. G. Kazovsky, "High-nonlinearity fiber optical parametric amplifer with periodic dispersion compensation," J. Lightwave Technol. **17**(2), 210–215 (1999).

#282544 https://doi.org/10.1364/OE.25.004810
Journal © 2017 Received 16 Dec 2016; revised 27 Jan 2017; accepted 30 Jan 2017; published 22 Feb 2017

Optics EXPRESS

15. C. Fourcade-Dutin, Q. Bassery, D. Bigourd, A. Bendahmane, A. Kudlinski, M. Douay, and A. Mussot, "12 THz flat gain fiber optical parametric amplifiers with dispersion varying fibers," Opt. Express **23**(8), 10103–10110 (2015).
16. J. Hansryd and P. A. Andrekson, "Broad-band continuous-wave-pumped fiber optical parametric amplifier with 49-dB gain and wavelength-conversion efficiency," IEEE Photonics Technol. Lett. **13**(3), 194–196 (2001).
17. L. Provino, A. Mussot, E. Lantz, T. Sylvestre, and H. Maillotte, "Broadband and at parametric amplifers with a multisection dispersion-tailored nonlinear ber arrangement," J. Opt. Soc. Am. B **20**(7), 1532–1537 (2003).
18. S. Takasaka, Y. Taniguchi, M. Takahashi, J. Hiroichi, M. Tadakuma, H. Matsuura, K. Doi, and R. Sugizaki, "Quasi phase-matched FOPA with 50 nm gain bandwidth using dispersion stable highly nonlinear fiber," in *Optical Fiber Communication Conference*, OSA Technical Digest (online) (Optical Society of America, 2014), paper W3E.2.
19. Y. Taniguchi, J. Hiroishi, M. Takahashi, and R. Sugizaki, "Nonlinear optical fiber, nonlinear optical device, and optical signal processor," European Patent 1988411A1 (2008).
20. A. E. El-Taher, J. D. Ania-Castañón, V. Karalekas, and P. Harper, "High efficiency supercontinuum generation using ultra-long Raman fiber cavities," Opt. Express **17**(20), 17909–17915 (2009).
21. V. Gordienko, M. F. C. Stephens, and N. J. Doran, "Novel broadband gain-spectrum measurement technique for Raman and parametric amplifiers," in *Optical Fiber Communication Conference* 2017, paper W2A.11.
22. R. H. Stolen, W. J. Tomlinson, H. A. Haus, and J. P. Gordon, "Raman response function of silica-core fibers," J. Opt. Soc. Am. B **6**(6), 1159–1166 (1989).
23. J. Hansryd, P. A. Andrekson, M. Westlund, Jie Li, and P.-O. Hedekvist, "Fiber-based optical parametric amplifiers and their applications," IEEE J. Sel. Top. Quantum Electron. **8**(3), 506–520 (2002).
24. F. Yaman, Q. Lin, S. Radic, and G. P. Agrawal, "Impact of dispersion fluctuations on dual-pump fiber-optic parametric amplifiers," IEEE Photonics Technol. Lett. **16**(5), 1292–1294 (2004).
25. M. F. C. Stephens, A. Redyuk, S. Sygletos, I. D. Phillips, P. Harper, K. J. Blow, and N. J. Doran, "The impact of pump phasemodulation and filtering on WDM signals in a fibre optical parametric amplifier," in *Optical Fiber Communication Conference*, OSA Technical Digest (online) (Optical Society of America, 2015), paper W2A.43.
26. Z. Tong, A. Bogris, M. Karlsson, and P. A. Andrekson, "Full characterization of the signal and idler noise figure spectra in single-pumped fiber optical parametric amplifiers," Opt. Express **18**(3), 2884–2893 (2010).

1. Introduction

The fiber optical parametric amplifier (FOPA) is an optical amplifier with the potential to increase the capacity of wavelength-division-multiplexing (WDM) transmission systems by providing wideband gain at arbitrary wavelengths [1,2]. The underlying process of the FOPA is based on four-wave mixing (FWM) which provides significant scope for obtaining low gain variation (GV) 'flat' unfiltered spectra compared with single pump Raman and Erbium-doped amplifiers [3]. Low unfiltered GV is important in a FOPA because nonlinear crosstalk scales as the square of the output signal power [4]. FOPAs with high GV are therefore likely to suffer from signal quality degradation arising from both higher crosstalk and additional noise associated with overcoming gain flattening filter loss. Other particular FOPA-specific features are: symmetrical gain around a central frequency f_c and the emergence of phase conjugate idlers possessing symmetry with any amplified signals about f_c [1]. Idler generation therefore typically constrains WDM signal gain within a FOPA (single or dual-pumped) to one side of f_c and this will be the assumption of this paper when defining gain bandwidth and comparing other reported results. Note that for a single-pump FOPA, f_c coincides with the pump frequency [1].

The FWM amplification efficiency is defined by phase matching and particularly by the propagation constant mismatch $\Delta\beta$ [5], so a common approach towards obtaining low GV broadband parametric gain relies on managing the spectral profile of $\Delta\beta$ within a highly nonlinear fiber (HNLF). It has been shown that $\Delta\beta$ is governed principally by the second- and the fourth-order derivatives (β_2 and β_4) of the propagation constant at f_c [1]. By tuning f_c near the zero dispersion wavelength λ_0 it is possible to find a value of β_2 which can compensate for the impact of the β_4-term on $\Delta\beta$ to obtain nearly perfect phase-matching over a large bandwidth [1,6]. This approach has been experimentally demonstrated using two-pump FOPAs operating with gains of 25 ± 1.5 dB over 7.1 THz (59 nm) [7], 23.5 ± 1.5 dB over 8.6 THz (73.5 nm) [8] or 38.5 ± 1 dB over 4.9 THz (39 nm) [9]. However two-pump FOPAs can be considered experimentally complex, suffer from significant 'unwanted' FWM, and require

Optics EXPRESS

high power pump generation in unfavorable parts of the spectrum to obtain wide bandwidth. Single pump FOPAs conversely can generate wide bandwidth using a pump placed in the C- or L-band where high power is easily obtainable. The achievable bandwidth is additionally not bound by the wavelength location of the pump, and the 'unwanted' FWM is substantially lower than the two-pump case [10]. The most notable single-pump FOPA achievements obtained with standard HNLF include gains of 12.3 ± 0.6 dB over 6 THz (50 nm) [11] and 16.8 ± 2.8 dB over 12.5 THz (110 nm) [12]. A number of alternative techniques to obtain a broadband flat single-pump FOPA gain spectrum have also been suggested [13–17]. One of them, using dispersion-varying HNLF, has enabled experimental demonstration of 63 ± 3.5 dB gain over 12 THz bandwidth in the 1100 nm region [15]. However, the viability of this technique has not been verified as of yet within the low-loss window of standard transmission fiber. Another promising technique, quasi-phase matching, has been used to experimentally demonstrate a gain of 23.7 ± 1.3 dB over 6.4 THz (50 nm) [18].

In this paper we experimentally optimize a single-pump FOPA gain spectrum to obtain a significant improvement of bandwidth and GV compared to the above achievements by tuning the pump wavelength around the λ_0 of a dispersion-stable HNLF possessing a positive value of β_4. We report a pure parametric gain bandwidth of >10 THz with GV below 1 dB. Moreover, we experimentally demonstrate for the first time that parametric and Raman gain spectra induced by the same pump may be merged together to obtain enhancement of the total gain bandwidth, whilst maintaining low GV. As a result we demonstrate a record flat and broad unfiltered single-pump Raman-enhanced FOPA gain spectrum with a GV of 1 dB over a continuous range of 111 nm (~12.9 THz) on one side of the pump. Figure 1 visually displays this result in context with the state-of-the-art achievements discussed above. GV normalized per 10 dB gain is introduced in this figure to allow a fair comparison of FOPAs with different gain. It can be seen that we report the largest gain bandwidth whilst achieving very low normalized GV. We additionally demonstrate the viability of the FOPA for signal amplification by amplifying a 60 Gbit/s QPSK signal at three different wavelengths across the L-band. We report an OSNR penalty of <1 dB for received Q^2 <14 dB compared to a back-to-back (B2B) unamplified configuration.

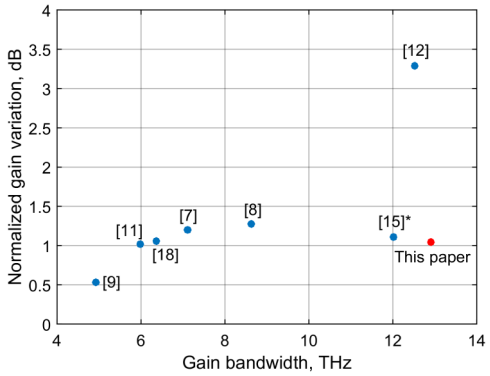

Fig. 1. Normalized gain variation (gain variation per 10 dB gain) versus gain bandwidth on one side of the FOPA central frequency f_c. Blue dots correspond to some of the most notable achievements experimentally demonstrated with FOPA. Numbers in square brackets denote references in this paper. The red dot corresponds to the gain spectrum reported in this paper (see below, 9 W). *This FOPA was not designed for signal amplification as it employed a non-CW pump in the 1100 nm region. It is therefore not directly comparable and is included for completeness.

2. Experimental setup

Figure 2 shows the experimental setup. A continuous pump wave generated from a 100 kHz linewidth tunable laser was phase modulated with RF tones at 100 MHz, 320 MHz and 980

Optics EXPRESS

MHz to mitigate stimulated Brillouin scattering (SBS). The pump was amplified by a high-power Ytterbium-Erbium Doped Fiber Amplifier (EDFA) and filtered using a circulator and tunable fiber Bragg grating (FBG) to remove ASE noise, and to combine the filtered pump with a chosen input signal. The pump and signal were guided into either 25 m or 50 m of dispersion-stable HNLF [19], derived from the same parent spool. The key datasheet parameters of the parent spool were: λ_0 = 1551 ± 0.5 nm, nonlinear coefficient γ = 14 $W^{-1}\cdot km^{-1}$, dispersion slope S = 0.044 $ps\cdot nm^{-2}\cdot km^{-1}$ and fourth order propagation constant β_4 ~10^{-56} $s^4\cdot m^{-1}$, measured at 1550 nm. Due to variation of dispersion parameters along the parent spool these values may be used for reference only. The λ_0 of the two experimentally investigated HNLF lengths will be discussed specifically in Section 3.

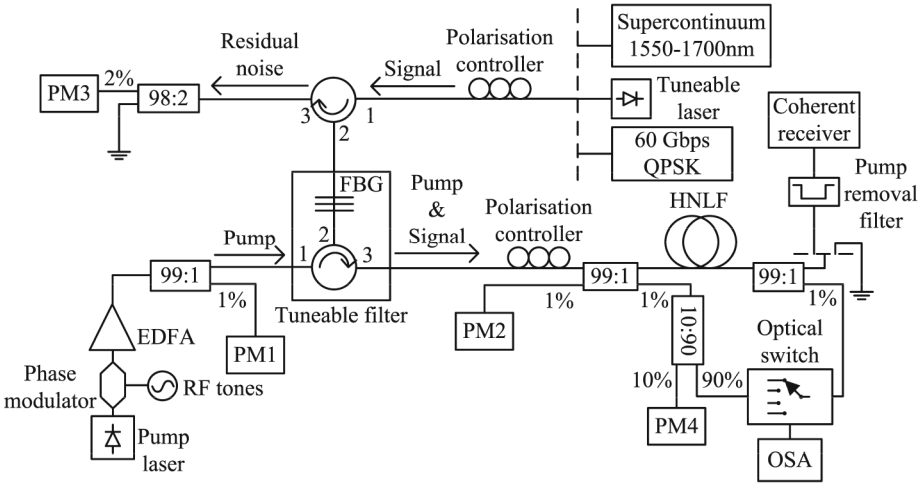

Fig. 2. Schematic of experimental setup.

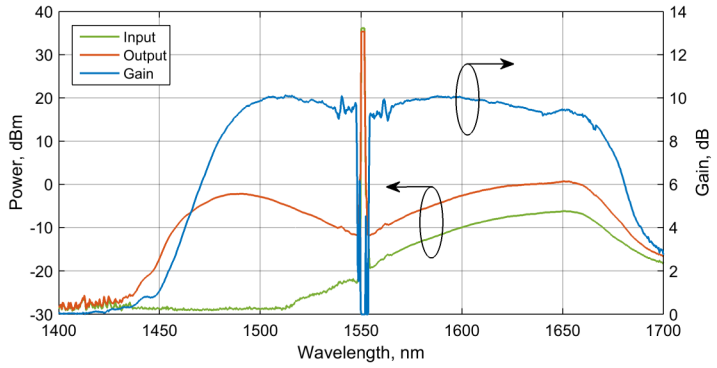

Fig. 3. Example optical spectra measured at the input and the output of HNLF with SC as a probe. Calculated gain spectrum is also shown. Fiber length was 25 m, pump wavelength was 1551.6 nm, pump power was 9 W and OSA resolution bandwidth was 2 nm.

Three variants of input source were used in this experiment: 1) a depolarized broadband supercontinuum (SC) source [20], ranging from 1520 nm to 1700 nm (Fig. 3); 2) a 100 kHz tunable laser (TL) operating in a range from 1570 nm to 1610 nm; 3) a wavelength-tunable 60 Gbit/s QPSK signal. The pump polarization was controlled after coupling with the signal to avoid changes in pump power with polarization due to polarization sensitivity of the FBG. A calibrated set of tap couplers and power meters (PMx) and an optical spectrum analyzer (OSA) were used to non-intrusively measure pump power and optical spectra at the input and output of the HNLF. The gain spectrum was calculated as the difference between output and

Optics EXPRESS

input spectra. In the depolarized SC case, the gain spectrum was scaled assuming that only half of the input signal was co-polarized with the pump and hence amplified [21]. In order to also ensure consistent measurement between gain spectra, the pump polarization was always tuned to maximize parametric gain, even if this led to higher GV. It was also ensured that gain spectra obtained with the SC were not distorted by pump depletion or 'unwanted' FWM by attenuation of the input until the measured gain was independent of input power. Results of all measurements therefore yield the small signal gain. Example power spectra measured at the input and the output of the HNLF and the corresponding calculated gain spectrum are shown in Fig. 3. Note that signal gain G_s on the anti-Stokes side of the pump was estimated based on symmetric idler gain G_i as $G_s = G_i + 1$ [1], because there was no input probe in this wavelength range.

3. Experimental results and discussion

Figure 4 shows experimental FOPA gain spectra obtained using the SC as signal for the (a) 25 m and (b) 50 m fibers at 5 W pump power for pump wavelengths λ_p varied in a range from 1550 nm to 1556 nm. Gain spectra are plotted versus frequency relative to the pump to avoid a shift between curves that would arise within the wavelength domain. We additionally show gain spectra measured using the TL for the 50 m fiber at two pump wavelengths: λ_p = 1551.4 nm and λ_p = 1556 nm. The TL shows excellent agreement with the SC source, validating the use of the latter for accurate prediction of polarized signal gain. A detailed full bandwidth comparison is reported in [21].

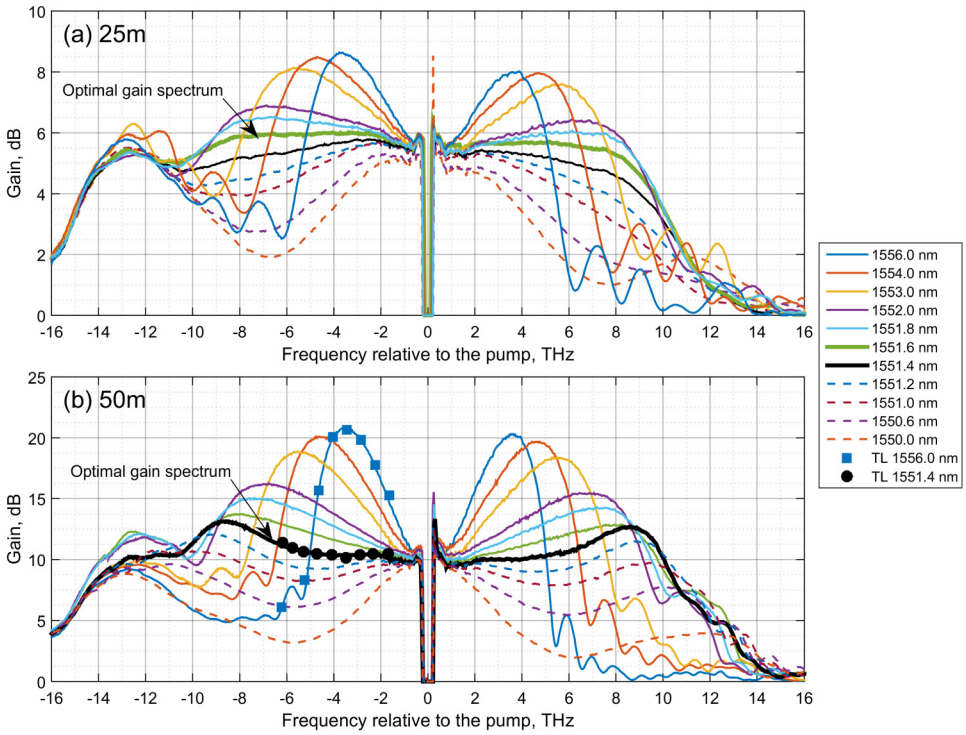

Fig. 4. Experimental FOPA gain spectra for a range of pump wavelengths and a pump power of 5 W for a) 25 m and b) 50 m HNLF. Lines are obtained using the SC and markers using the TL. Different line styles are to visually distinguish different curves.

It can be seen that the total gain bandwidth is over 28 THz, including over 16 THz on the Stokes (lower frequency) side, where amplification beyond 11 THz from the pump is attributed to forward Raman gain. This is confirmed by the gain relative to the pump in this

Optics EXPRESS

region being independent of pump frequency and not being mirrored on the anti-Stokes side [22]. We concentrate here on the Stokes side performance owing to the larger gain bandwidth.

The gain spectra obtained with λ_p = 1551.6 nm for the 25 m fiber and at λ_p = 1551.4 nm for the 50 m fiber (highlighted in Fig. 4) possess an almost constant gain in a large area around the pump. As a result they have the lowest GV across the parametric gain window compared to other gain spectra obtained with corresponding fiber lengths. Moreover, the bandwidths of these gain spectra stretch over 11 THz allowing them to merge with forward Raman gain concurrently generated via the same pump. Therefore, λ_p = 1551.6 nm (25 m) and λ_p = 1551.4 nm (50 m) may be considered the optimal GV pump wavelengths.

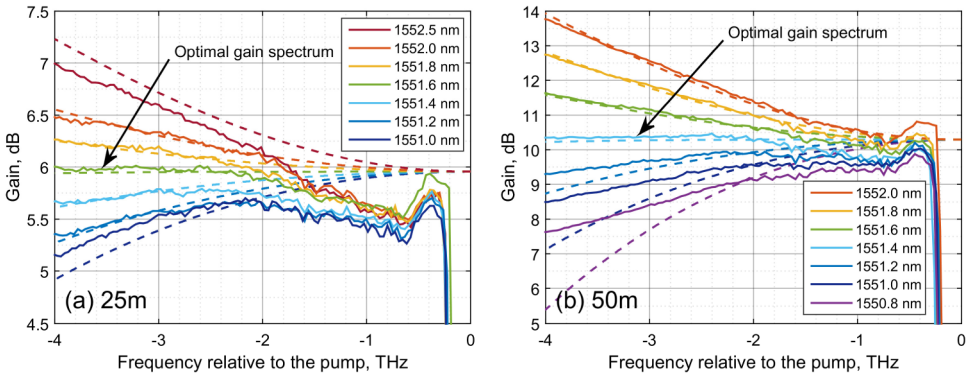

Fig. 5. Theoretical FOPA gain spectra (dashed) and experimental (solid) curves for a) 25 m and b) 50 m fibers. Theoretical gain spectra are calculated with following parameters: a pump power of 5 W, S = 0.044 ps·nm^{-2}·km^{-1}, β_4 = 10^{-56} s^4·m^{-1} and a) λ_0 = 1551.6 nm, γ = 13.7 W^{-1}·km^{-1} and b) λ_0 = 1551.4 nm, γ = 12.5 W^{-1}·km^{-1}.

To help understand the relationship of these optimal GV pump wavelengths to the λ_0 of each HNLF, Fig. 5 displays both experimental and theoretical FOPA gain curves as the pump is tuned about the optimal values. The theoretical gain is plotted using the datasheet HNLF parameters listed earlier and according to:

$$G_s = 1 + \left[\frac{\gamma P}{g}\sinh(gL)\right]^2, \tag{1}$$

where P is pump power, L is fiber length, and g is a gain coefficient dependent on $\Delta\beta$ [1]. It should be noted that Eq. (1) is based on standard FOPA scalar theory and neglects fiber loss, pump depletion, polarization and Raman gain. For the theoretical curves, λ_0 is set to the experimentally-obtained optimal GV pump wavelength for each fiber. It can firstly be seen that the experimental results close to the pump (0-2 THz) are distorted and need to be discounted from this analysis – the distortion is due to imperfect filtering of residual ASE from the pump EDFA. The gradient of the theoretical gain curves can be seen to change from positive to negative as the pump wavelength is tuned from wavelengths longer than λ_0 (anomalous dispersion) to shorter (normal dispersion). Generally good agreement between experiment and theory is seen in the 2-4 THz region which strongly implies that the optimal GV pump wavelength is close (within measurement granularity and error) to the λ_0 of each fiber. Therefore we estimate λ_0 = 1551.6 ± 0.1 nm and λ_0 = 1551.4 ± 0.1 nm for the 25 m and 50 m fibers respectively. It should be noted that at frequencies extending beyond 4 THz there is significant divergence of the theory from experimental observation which is attributed primarily to insufficient knowledge of the HNLF dispersion profile, impact of polarization effects and the Raman contribution. This will be addressed in future extended simulation work.

Optics EXPRESS

Within silica fiber, the Raman gain coefficient is much lower than the phase-matched parametric gain coefficient [23]. This experiment demonstrates however that phase-mismatched parametric gain can be adjusted to be at the same level as the Raman gain. Therefore, if the parametric gain roll-off is countered by a corresponding rise of the Raman gain, they can be utilized together to keep the overall GV low with extremely wide overall bandwidth.

Figure 6 shows gain spectra obtained for both fibers using the optimal GV pump wavelengths for a range of pump powers from 4 W to 9 W. It shows that increasing the pump power above 5 W for the 50 m fiber causes an exponential growth of the gain peak, which is deleterious to GV. This does not occur in the 25 m fiber as it can be seen that an increase of the pump power up to 9 W provides an ultra-flat gain spectrum of 9.6 ± 0.5 dB in a range of 111 nm (12.8 THz). It should be noted that although the pump powers may be considered high in this work, if the amplifier is to be used to amplify typical telecoms signals across the full band then signal output powers will be in the Watt region. This implies that any next-generation wideband optically pumped amplifier will require multi-Watt pumps.

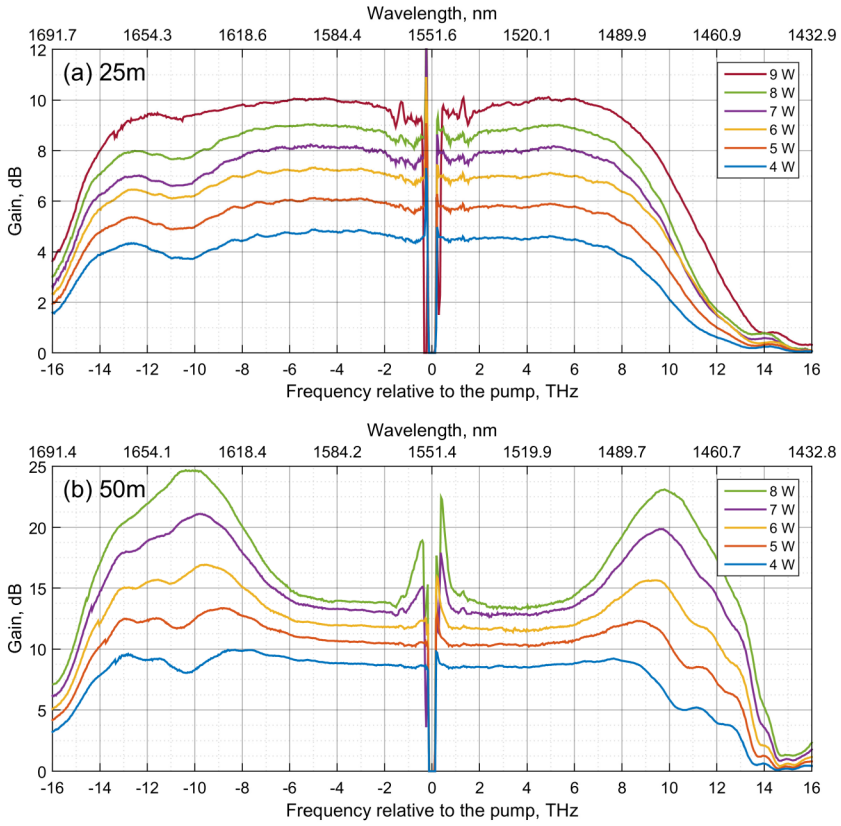

Fig. 6. Experimental FOPA gain spectra for a series of pump power values at optimal pump wavelength for a) 25 m HNLF (λ_p = 1551.6 nm) and b) 50 m HNLF (λ_p = 1551.4 nm). All curves are obtained with a SC.

A direct comparison of the two fibers for equivalent gain levels is shown in Fig. 7, where the 25 m fiber was pumped with twice the power compared to the 50 m to achieve the same nonlinear phase shift (γPL) for both. The first observation is that there is a clear scaling of gain with γPL. For the higher 9 dB gain case, the 50 m fiber spectrum exhibits a small peak which is not observed in the 25 m fiber. In the case of 6 dB gain this peak is not evident, but the GV is still higher for the 50 m fiber. This is due to the reduced pump power (2.5 W)

Optics EXPRESS

causing a reduction in parametric gain bandwidth which produces a gap between the parametric and Raman bands at 10 THz. Overall, the 25 m fiber shows less GV for the same gain value in both cases because it is not degraded by longitudinal fluctuations of the dispersion parameters [24]. The total gain bandwidth is the same for both fibers as it is limited by the Raman contribution in both cases.

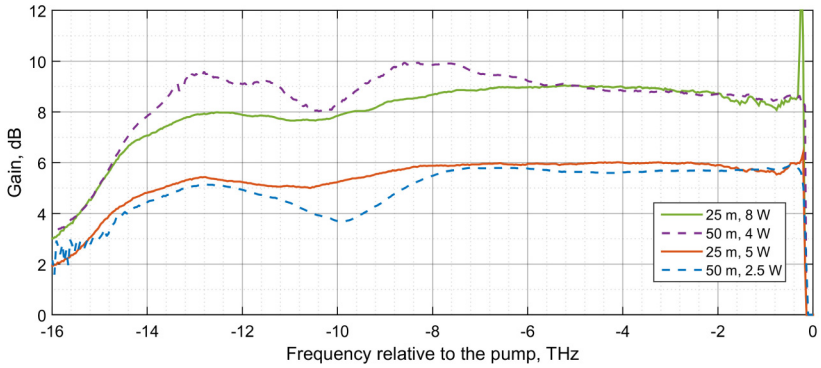

Fig. 7. Comparison of experimental FOPA gain spectra obtained at optimal pump wavelengths with 50 m (λ_p = 1551.4 nm) and 25 m (λ_p = 1551.6 nm) fibers for equal gain level.

Even though the absolute gain magnitude demonstrated in this paper might not be considered large (~10 dB), we envisage cascading two of these FOPAs at optimum GV with pump reuse and idler removal in the second stage to increase overall gain. Considering that the normalized GV of the reported FOPA is one of the lowest of Fig. 1, the cascaded setup is anticipated to also have a low normalized GV, while maintaining a superior gain bandwidth.

4. Experimental signal amplification

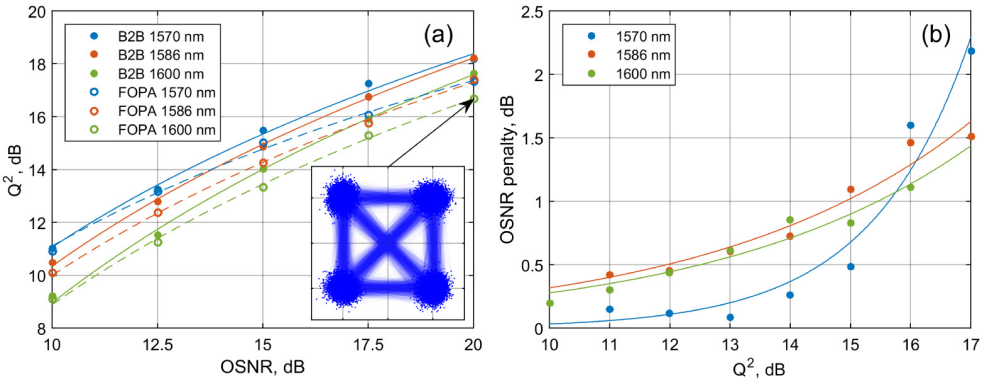

Fig. 8. Comparison of 60 Gbit/s QPSK signal performance at three signal wavelengths in B2B configuration and after 9 dB amplification by the 25 m FOPA. (a) Q^2 versus OSNR for B2B configuration (filled circles and solid trend lines) and after amplification (empty circles and broken trend lines); an example constellation for the amplified signal is shown inset. (b) OSNR penalty for each signal wavelength (filled circles) with trend lines.

To ascertain the suitability of the demonstrated FOPA for use within telecommunication applications, a single-polarization 60 Gbit/s QPSK signal was amplified and the signal quality measured at three wavelengths of 1570 nm, 1586 nm and 1600 nm. The examined wavelength range was limited only by the test equipment used for analysis. The received signal OSNR was measured with a resolution bandwidth of 0.1 nm and varied from 10 dB to 20 dB by loading ASE noise from an L-band EDFA. Each signal was coherently detected and

Optics EXPRESS

digitally sampled using a real-time oscilloscope with 80 GHz sampling rate. Offline standard digital signal processing was used to count bit errors and to estimate a Q^2 value from the constellation when no bit errors were measured. The performance of signals amplified by 9 dB using the 25 m long HNLF and a pump wavelength and power of 1551.6 nm and 8 W respectively was compared with the B2B unamplified performance and is plotted in Fig. 8(a). The degradation of the B2B performance with increased wavelength is attributed to the wavelength dependent response of the transmitter modulator. OSNR penalty of the amplified signal relative to B2B was subsequently calculated and plotted in Fig. 8(b). Since there was no measurement points with exactly the same value of Q^2 for both B2B and FOPA configurations, a linear approximation of Q^2 vs OSNR was used to calculate OSNR penalty. It should be noted that the lines of Fig. 8 are merely best fits for visual guidance and have no physical relevance. The error in the penalty calculation was estimated to be 0.5 dB. OSNR penalties below 1 dB are observed for $Q^2 \leq 14$ dB, which are attributed primarily to dithering and noise transfer from the pump [25]. OSNR penalties at 1586 nm and 1600 nm are almost the same. OSNR penalty at 1570 nm for $Q^2 \leq 15$ dB is measured to be smaller, but the difference is within measurement error. The reason for the large increase of OSNR penalty seen at 1570 nm for $Q^2 > 15$ dB is unclear, but is speculated to be due to residual ASE noise from the EDFA amplifying the pump [26].

5. Conclusions

A single-pump, high-power and short-length FOPA was experimentally optimized in terms of gain spectral bandwidth and GV. It was found that parametric gain may be stretched over 11 THz with GV below 1 dB. This allows extension of the gain spectrum by merging the parametric spectrum with a forward Raman gain spectrum provided by the same pump. It was shown that the 25 m fiber provides a superior GV compared to 50 m for the same gain value and bandwidth and that optimal GV is achieved when the pump wavelength is tuned to the fiber ZDW. This was confirmed by theoretical gain calculations up to 4 THz from the pump. An ultra-flat gain of 9.6 ± 0.5 dB in a range of 111 nm (12.8 THz) was demonstrated with a 25 m of dispersion-stable HNLF and pump power of 9 W. OSNR penalty less than 1 dB was observed for a 60 Gbit/s QPSK L-band signal for received Q^2 below 14 dB. We believe the absolute gain magnitude for this FOPA may be further improved whilst maintaining a similarly low GV to gain ratio and wide bandwidth by employing two-stage amplification in this regime with pump-reuse and idler removal. This work is therefore a promising step towards an ultra-wideband, low GV FOPA for future broadband systems.

Funding

Engineering and Physical Sciences Research Council (EPSRC) (EP/M005283/1, EP/J017582/1).

Acknowledgments

The authors wish to thank Dr Shigehiro Takasaka, Dr Ryuichi Sugizaki (both Furukawa Electric Co.) and Dr Ian McClean (II-VI) for useful discussions. The fibers used in this work were kindly provided by Furukawa Electric Co. V. Gordienko is thankful to II-VI for CASE support. The experimental and theoretical data contained within this paper are available for download at: http://doi.org/10.17036/researchdata.aston.ac.uk.00000171.